The effects of an aggressive breast tumor on thrombosis after antithrombin downregulation in a hypercoagulable mouse model

Ünlü, B.; Heestermans, M.; Laghmani, E.; Buijs, J.T.; Akker, R.F.P. van den; Vlijmen, B.J.M. van; Versteeg, H.H.

Thrombosis Research 244 (2024) 109200

Contents lists available at ScienceDirect

Thrombosis Research

journal homepage: www.elsevier.com/locate/thromres

Full Length Article

The effects of an aggressive breast tumor on thrombosis after antithrombin downregulation in a hypercoagulable mouse model

Betül Ünlü, Marco Heestermans, El Houari Laghmani, Jeroen T. Buijs, Rob F.P. van den Akker, Bart J.M. van Vlijmen, Henri H. Versteeg *

Einthoven Laboratory for Vascular and Regenerative Medicine, Division of Thrombosis and Hemostasis, Department of Internal Medicine, Leiden University Medical Center, Leiden, the Netherlands

ARTICLE INFO

Keywords:
Venous thromboembolism
Mice
RNA interference
Animals
Antithrombin
Breast cancer
cancer-associated thrombosis
Fibrin
VTE

ABSTRACT

Background: Despite improvements in therapy, breast cancer still contributes to high mortality rates. Survival of these patients becomes progressively worse upon diagnosis with cancer-associated thrombosis (CAT). Unfortunately, the mechanism causing CAT has remained unclear.
Objective: Set up an acute and non-invasive hypercoagulable mouse model with an aggressive breast cancer and study the mechanism of cancer-associated thrombosis.
Methods: Mice were grafted with the aggressive breast cancer cell line MDA-MB-231 or sham-treated. Subsequently, an acute imbalance in coagulation was introduced by injecting a synthetic small interfering (si) RNA targeting hepatic *Serpinc1* to knockdown antithrombin – a condition known to predispose to cause a hypercoagulant state *in vivo*.
Results: Silencing *Serpinc1* with siRNA decreased plasma antithrombin levels. siRNA treatment had no short-term effects on tumor characteristics, but increased distant metastasis within the timeframe of this study. The systemic pro-inflammatory status, with elevated platelet counts and fibrinogen levels in tumor-bearing mice, was also not affected by antithrombin silencing. While elevated fibrin deposition in the liver upon *Serpinc1* targeting was not significantly affected by the presence of breast cancer, knockdown of antithrombin did significantly increase intratumoral fibrin deposition and inflammation. Surprisingly, in the presence of an aggressive tumor, a protective outcome with less clinical features coinciding with venous thrombosis were observed in mice with antithrombin knockdown.
Conclusion: We conclude that the presence of a breast tumor protects hypercoagulant mice from severe consumption of coagulation factors after lowering hepatic antithrombin levels, possibly due to elevated platelet counts. However, the consequences on cancer-associated thrombosis remained inconclusive.

1. Introduction

One in eight women will be diagnosed with breast cancer in their lifetime. In addition, it is estimated that over 300.000 new invasive breast cancer cases will be reported in 2024 in the United States [1]. Despite early detection and improved treatment over the last decade, breast cancer is still ranked among the cancer types with high mortality rates [2]. Survival of breast cancer patients is further reduced when these patients are presented with cancer-associated thrombosis (CAT). The risk of venous thromboembolism (VTE) in patients with breast cancer is increased 3–4-fold when compared to women that are not diagnosed with breast cancer [3–5]. Among all breast cancer patients, the relative incidence of CAT is around 1–2 % and is therefore generally categorized as a cancer type with a low risk of CAT [6]. However, the absolute number of VTE events in breast cancer is high as i) metastasis dramatically increases the risk of CAT [7] and ii) breast cancer is one of the most frequently diagnosed types of cancer [8]. For these reasons, up to 17 % of all CAT cases are breast cancer-related [3,9]. While studies have revealed that most cancer patients have a procoagulant state [10–12] this does not necessarily lead to formation of a thrombus, the reasons for which are unknown. This poor understanding of the mechanism underlying CAT makes it challenging to predict which cancer patient will develop CAT and which patient might benefit from prophylactic anticoagulant treatment.

* Corresponding author at: Department of Internal Medicine, Leiden University Medical Center, 2333 ZA Leiden, the Netherlands.
E-mail address: h.h.versteeg@lumc.nl (H.H. Versteeg).

https://doi.org/10.1016/j.thromres.2024.109200
Received 4 February 2024; Received in revised form 22 October 2024; Accepted 22 October 2024
Available online 23 October 2024

To understand the mechanism of CAT, various *in vivo* models have been developed trying to mimic the clinical setting. Mice do not spontaneously develop VTE, therefore it needs to be provoked, reviewed by Diaz et al. and Hisada et al. [13,14]. The most common methods are infrarenal vena cava ligation, or exposure of the vessel to laser irradiation. So far, for all commonly used approaches mice must undergo surgical procedures. Besides the method of thrombosis provocation, the tumor type and location in mice are equally important, as nicely reviewed by Palacios-Acedo and colleagues [15]. Unfortunately, the combination of VTE and cancer models in mice have their limitations. Therefore, attention must be paid to make sure important aspects that contribute to CAT are present in the model of choice, such as endothelium activation, immune system involvement, tumor microenvironment modulation and metastasis [15]. In our department we have developed a non-invasive experimental mouse model in which spontaneous thrombosis follows siRNA-mediated (acute) downregulation of antithrombin (*Serpinc1*) expression in the liver together with Protein C (*Proc*) downregulation. Similarly, knockdown of antithrombin only also results in venous thrombosis although a milder phenotype was observed, when compared to the combined knockdown of antithrombin (AT) and Protein C [11]. This imbalance of coagulation triggered by downregulation of antithrombin in the presence or absence of simultaneous Protein C downregulation causes occlusive venous thrombi, with layers of fibrin, in the mandibular area of the head of these mice within days after siRNA administration. Thrombus formation is dependent on thrombin, platelets and tissue factor (TF), while plasma analysis shows prolonged prothrombin and activated partial thromboplastin time [16]. Additionally, the mice feature consumption of platelets, tissue fibrin deposition in the liver and periocular hemorrhaging secondary to the thrombus formation in the head. However, fibrinogen levels in the plasma are not affected [11]. In addition, this approach towards a non-invasive thrombosis model with reduced antithrombin levels, resulting in a prolonged systemic hypercoagulable state in NOD-SCIDγ mice, did not affect breast tumor progression [17]. As previously mentioned, mice do not develop thrombi spontaneously, even in the presence of an aggressive tumor. Additionally, *in vitro* experiments do not yield a comprehensive picture of all the processes related to the mechanism of cancer-associated thrombosis. Therefore, in this study we reciprocally examined the impact of an aggressive breast cancer on thrombus formation in mice using our acute, non-invasive hypercoagulable model with downregulated antithrombin expression levels. We unexpectedly demonstrate that the presence of breast cancer alleviates the hypercoagulant phenotype, when tumor bearing mice were compared to cancer-free mice.

2. Methods

2.1. Animal experiments

All the animal experiments were approved by the animal welfare committee of the Leiden University Medical Center (LUMC). Based on our previous paper, with fibrin deposition in tissues as a result of siRNA treatment, our power calculation was as follows: siRNA increases fibrin deposits by 2.5-fold, with and SD of 50 %. For a power of 80 % and an alpha of 0.05, the group size must consist of 6 mice per condition [17]. At the D1 level biosafety laboratory, six mice per sterile GM500 cage were housed with bedding material and a paper cylinder roll for cage enrichment. Water and food were available *ad libitum* and cages were refreshed on a weekly basis. Upon arrival to the animal facility of the LUMC, mice were randomly divided into three groups of six mice per cage, marked on the tail with a permanent marker, and allowed acclimatization for 1 week. Throughout the experiments, researchers were not blinded to the treatments. Orthotopic injections of tumor cells were performed as described previously [18]. Mice were anesthesized using 2.5 % isoflurane at 2–3 l/min O2, and kept on a heating pad during surgery to prevent hypothermia. In brief, 5×10^5 MDA-MB-231-pcDNA-GFP-lung cells or 50 μl serum free media (Sham) were injected into inguinal fat pads of 6-week-old female NOD-SCIDγ mice (Charles River, Wilmington, MA, USA); as an analgesic 0.1 mg/kg temgesic (Schering-Plough, Kenilworth, NJ, USA) was injected. The tumor dimensions were measured with a caliper, recording both length (L) and width (W). Volume was calculated with the formula $V = (LxW^2)/2$. Additionally, tumors were carefully dissected and weighed at the end of the experiment. After each measurement, the cages were placed randomly in the rack of the cage housing. When tumors reached ~400 mm^3, the siRNA-mediated silencing of antithrombin was initiated, essentially as previously described [11]. In short, siRNAs targeting antithrombin (si*Serpinc1*; cat. #S62673; Ambion, Carlsbad, CA, USA) or control (si*NEG*; cat #4404020; Ambion, Carlsbad, CA) were complexed with Invivofectamine 3.0 (Invitrogen, Carlsbad, CA, USA) and 1.2 mg siRNA/kg of body weight was injected intravenously *via* the tail vein. Citrated (tail) blood was collected 1 day prior to xenograftment, siRNA treatment and at the indicated end point (sacrifice). After siRNA treatment, mice were weighed and monitored twice a day to look for signs of discomfort *e.g.* >20 % weight loss, ruffled fur, reduced mobility and signs of bleeding from the eye. Mice were sacrificed as soon as i) the periocular hemorrhage sign was observed which was at either day 3 or day4 post siRNA injection, ii) or 4 days post siRNA injections. No mice were excluded from analysis.

Four days after tail vein injections, before mice were anesthetized and citrated (tail) blood was collected for blood analyses using a hematology analyzer (Sysmex XP-300; Sysmex Corporation, Kobe, JPN). To collect circulating tumor cells [19], 450 μl blood was drawn from the right atrium *via* heart puncture. After red blood cell lysis, cells were grown *ex vivo* for 1 week in 10 cm culture dishes, in DMEM supplemented with 10 % FBS, 2 mM L-glutamine and 1 % penicillin/streptomycin at 5 % CO_2, 37 °C. Furthermore, tumors, lungs and livers were collected, of which a part was snap-frozen in liquid nitrogen or fixed in 4 % formaldehyde. Mouse heads were collected and fixed in 4 % formaldehyde.

2.2. ELISA

Plasma antithrombin and fibrinogen protein levels were determined using commercial murine ELISA kits, according to manufacturer's protocol (Affinity Biologicals). Pooled plasma from mice was used for reference.

2.3. qPCR

To determine presence of human metastatic cancer cells in organs, a qPCR was performed with primers for human GAPDH (Fw: 5′-TTCCAGGAGCGAGATCCCT-3′; Rv: 5′-CACCCATGACGAACATGGG-3′) and mouse β-actin (Fw: 5′-AGGTCATCACTATTGGCAACGA-3′; Rv: 5′-CCAAGAAGGAAGGCTGGAAAA-3′). According to the manufacturer's protocol total organ RNA was isolated using Trisure (Bioline; Bio-38033; London, UK) and converted to cDNA using the Super script II kit (Life Technologies, Waltham, MA, USA). SYBR Select (Life Technologies, Waltham, MA, USA) was used to conduct qPCR on a CFX384 Touch real-time PCR detection system (BioRad, Veenendaal, the Netherlands). A list of all used primer sequences can be found in supplementary table 1.

2.4. Western blotting

Fibrin deposits in tumor and organs were determined using western blotting as described previously [20]. In brief, fibrin was extracted from tissue specimens, equal protein concentrations were loaded onto 4–12 % Bis-Tris Plus Gels (Thermo Fisher Scientific, Waltham, MA, USA) for 20 min at 200 V and blotted on 0.2 μm pore size PVDF membranes and blocked in 5 % milk in TBST (Tris-buffered saline with Tween-20) for 1 h at room temperature. Blots were incubated with mAb 59D8 (a kind gift from prof. C. Esmon, Oklahoma City, OK, USA) O/N at 4 °C, 3 TBST

washing steps and incubated with a horseradish peroxidase secondary anti-mouse antibody (Abcam, Cambridge, UK) at room temperature for 1 h. Peroxidase activity was visualized with Western Lightning Plus ECL (Perkin-Elmer, Waltham, MA, USA) using the ChemiDoc imaging system (BioRad, Veenendaal, The Netherlands). Band intensity was quantified by ImageJ software.

2.5. Immunohistochemical staining

Paraffin-embedded lung tissues were cut in 5-μm sections, deparaffinized, rehydrated and stained in Mayer's Hematoxylin for 1 min. After washes with tap water, tissues were dehydrated, counterstained for 2 min in 1 % Eosin and mounted. Images were taken using a microscope, at 1× and 20× magnifications.

2.6. Statistical analysis

Data are represented as mean and standard error of mean (SEM). Non-parametric testing was performed, comparisons between data points were done with Student's *t*-test for two conditions, or with 1way or 2way ANOVA for three or more data sets.

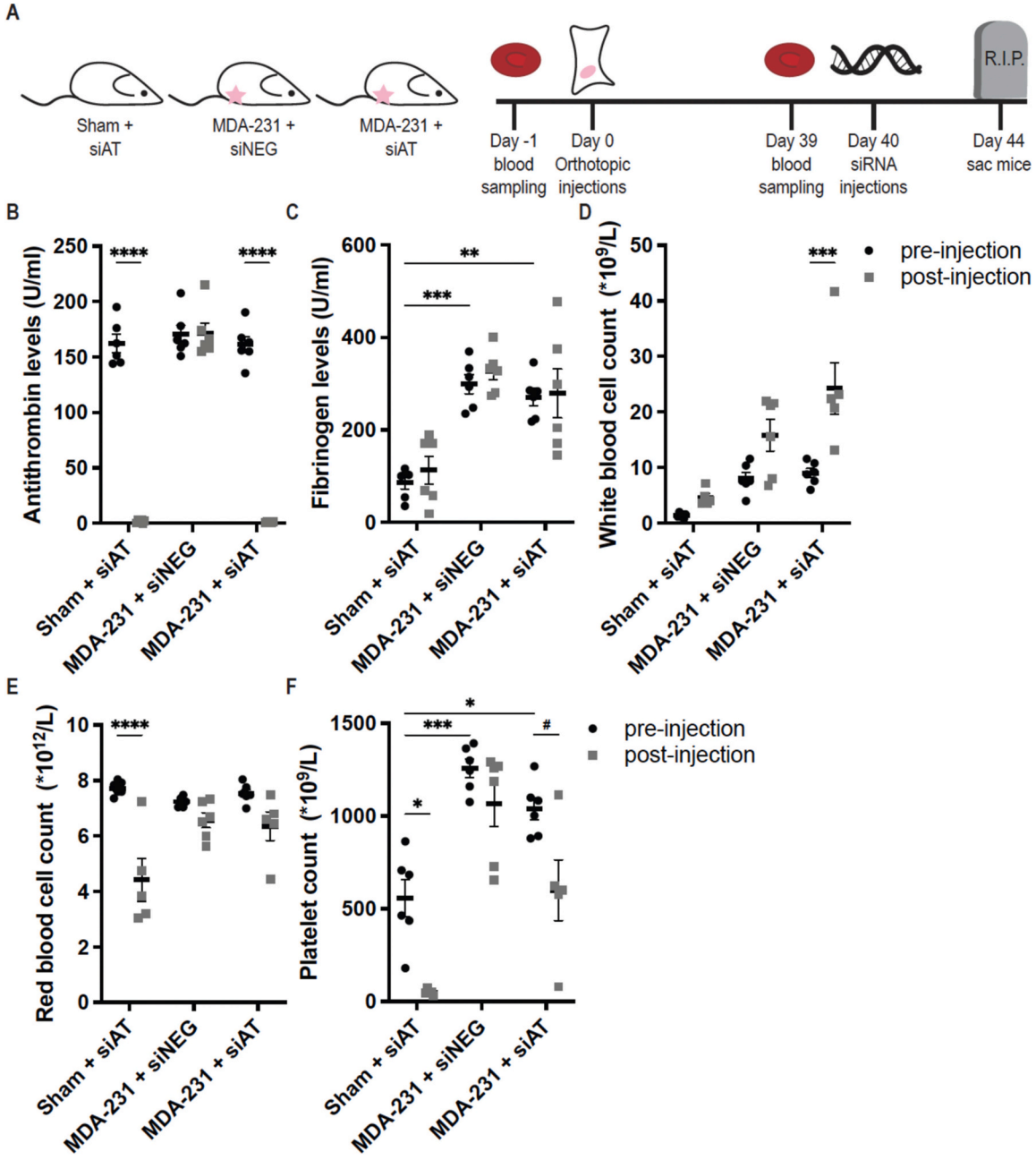

Fig. 1. Plasma analysis of NOD-SCIDγ mice before and after siRNA treatment. (A) A schematic overview of the experimental design. In total, three groups of mice were used ($n = 6$ per group), either injected with serum-free media (Sham) or with MDA-231 cells (indicated by a star). After 40 days (6 weeks), siRNAs were injected against antithrombin (siAT) or a negative control (siNEG). (B) At 4 days post injection mouse plasma analysis for antithrombin knockdown and (C) fibrinogen levels. (D) White and (E) red blood cell counts in whole blood before and after siRNA treatment. (F) Platelet levels at baseline (black) and consumed (grey) levels. # $P <$ 0.15, * $P < 0.05$, ** $P < 0.01$, *** $P < 0.001$, **** $P < 0.0001$. (siAT; si*Serpinc1*). (For interpretation of the references to colour in this figure legend, the reader is referred to the web version of this article.)

3. Results

To investigate if the presence of an aggressive breast tumor contributes to timing and morphology of thrombus formation, mice were Sham operated or xenografted with the highly aggressive subclone MDA-231-pcDNA-lung, which is a cell line that was previously reisolated from metastatic lung foci [21]. Six weeks after tumor engraftment, all mice received tail vein injections with siNEG (control) or siRNA siAT (*Serpinc1*), the latter resulting in a prominent and reproducible hypercoagulant state as shown before in our previous work [17], and were sacrificed after four days (Fig. 1A). After siRNA injections mice were closely monitored for signs of hemorrhages as a clinical feature coinciding with venous thrombosis. To verify knockdown, antithrombin plasma levels were analyzed. Indeed, a > 95 % reduction of antithrombin levels in plasma was confirmed 4 days post-injection, whereas control siNEG had no effect on plasma antithrombin levels after tail vein injections (Fig. 1B). The presence of an aggressive breast tumor had no effect on plasma antithrombin concentration (Fig. 1B). As reported earlier [11], no plasma fibrinogen consumption was detected in this thrombosis model in which only *Serpinc1* was targeted, although the presence of a tumor significantly increased overall fibrinogen levels 3-fold (Fig. 1C). Interestingly, white blood cell counts were elevated by 4-fold in mice bearing a tumor when compared to the Sham group. In addition, a significant increase in white blood cells was only observed in

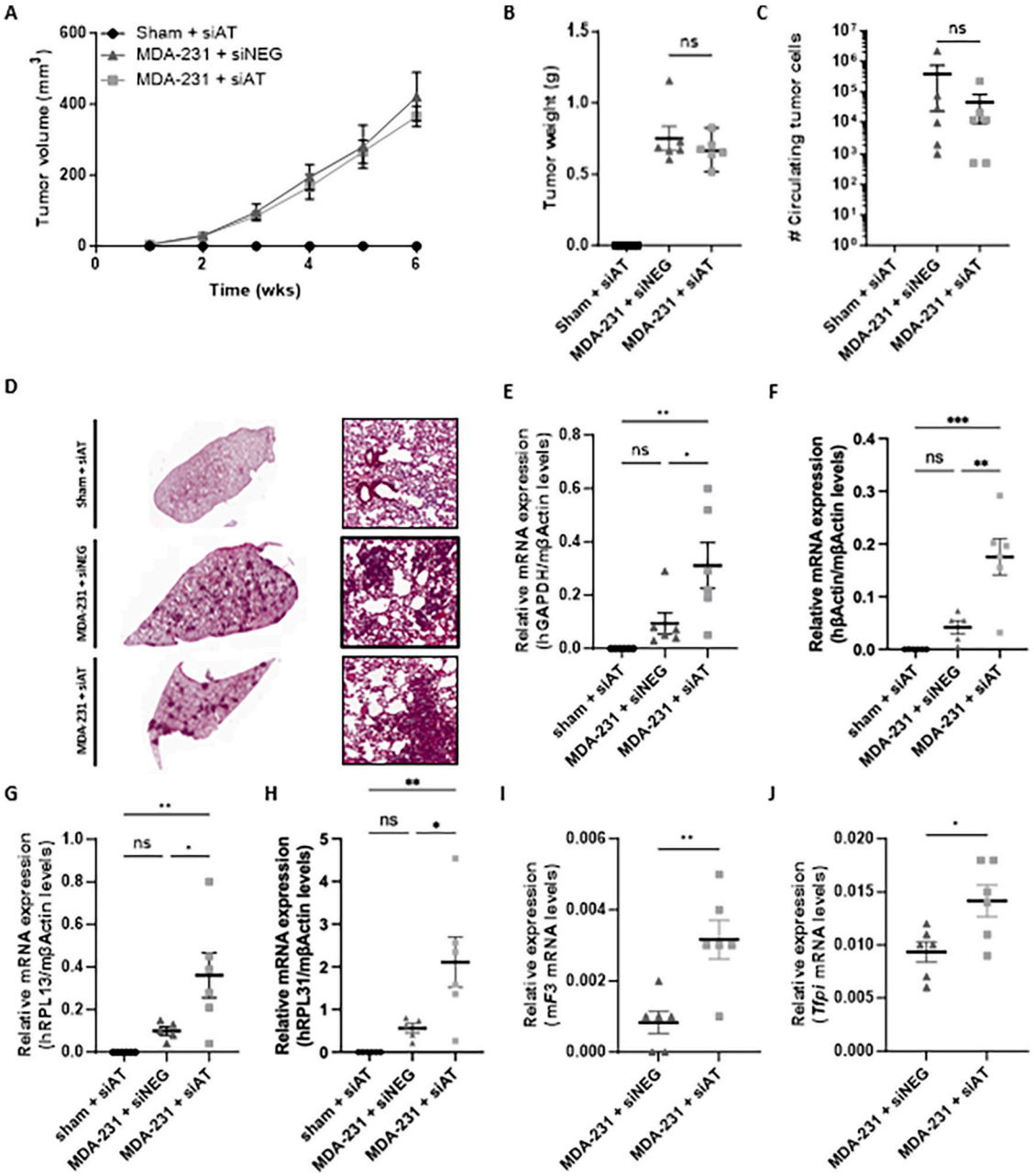

Fig. 2. Tumor characteristics of NOD-SCIDγ mice 4 days after siRNA tail vein injections. (A) Sham ($n = 6$) or tumor cells (n = 6 per siRNA treatment) were orthotopically injected and tumor volumes were monitored until week 6. (B) Tumor weight after mice were sacrificed. (C) The total amount of outgrown circulating cells *ex vivo* were counted. (D) H&E staining on lung tissue to address metastasis, shown on whole lung tissue (left panel) or 20× magnification (right panel). (E-F) Lung cells were isolated and micro-metastasis was assessed *via* qPCR, where human GAPDH (E), human β-actin (F), human RPL13 (G) or human RPL31 (H) was normalized to mouse β-actin levels. (G-H) mRNA expression levels of murine *F3* (G) and *Tfpi* (H) in tumors of mice injected with siAT or siNEG. NS = not significant, * $P < 0.05$, ** $P < 0.01$. (siAT; si*Serpinc1*).

tumor-bearing mice after siAT treatment, while in the Sham+siAT and MDA-231 + siNEG groups the increase in white blood cells did not reach significance (Fig. 1D). Furthermore, a 2-fold decrease of red blood cells was observed only in Sham+siAT mice in the absence of a tumor (Fig. 1E). Platelets were almost completely consumed in the Sham+siAT group, while a trend towards moderate platelet consumption was observed in mice with a tumor (Fig. 1F). Interestingly, baseline platelet levels were twice as high in mice with a tumor compared to those without cancer. We conclude that an efficient knockdown of antithrombin resulted in platelet consumption while fibrinogen levels remained unaffected, regardless of the presence of a tumor.

To investigate whether a hypercoagulant state had any short-term effects on malignancy, tumor characteristics were studied. No effects of siRNA treatment on tumor volume and weight were observed (Fig. 2A and B). Furthermore, similar numbers of circulating tumor cells were present in tumor-bearing mice treated with siAT or siNEG (Fig. 2C). Next, metastasis was addressed by performing hematoxylin and eosin (H&E) staining on lung tissue. We did not observe differences in large metastatic foci in lungs of mice that were grafted with MDA-231 cells and treated with siAT mice when compared to MDA-231-grafted mice that received siNEG treatment (Fig. 2D). Nevertheless, mice were sacrificed 4 days after siRNA treatment, which does not allow for outgrowth of small metastatic foci that cannot be visualized using immunohistochemistry. We therefore also used an established real-time PCR-based detection of metastasis [17], determining expression of 4 human cancer cell-derived mRNAs, normalized for mouse β-actin, representing mouse lung tissue. Using this method, we found a significant 3–4-fold increase in lung metastases in mice treated with siAT compared to siNEG (Fig. 2E-H). Lowered antithrombin levels did not affect the mRNA expression levels of Tissue Factor (*F3*) or Tissue Factor pathway inhibitor (*TFPI*) expressed by the tumors (SFig. 1A and D). Interestingly, murine TF (m*F3*) and *Tfpi* mRNA expression was increased in tumors of mice with siAT, suggesting adaptations of the host cells in the tumor microenvironment (Fig. 2I and J). Further analysis of lung and liver tissues showed no significant changes in mRNA expression between the groups (SFig. 1). These data show that siRNA treatment and targeted knockdown of antithrombin in the liver has no short-term effects on tumor growth but promoted micro-metastasis *in vivo*.

We investigated whether the presence of an aggressive tumor affected the formation of thrombosis *in vivo*. The typical clinical features secondary to thrombosis after siAT injection, as reported before [16,17], were detected in the head and consisted of periocular hemorrhaging (Fig. 3A). Five out of 6 mice presented clinical signs in the Sham+siAT group, whereas only 3 out of 6 mice had features coinciding with VT in the MDA-231 + siAT condition (Fig. 3B), albeit not statistically significant. As expected, none of the control mice (MDA-231 + siNEG) showed signs of these secondary bleedings. Further investigation of the tumors showed a significant pro-inflammatory status in tumor-bearing mice with reduced antithrombin levels when compared to siNEG treated mice (Fig. 3C-F). We finally investigated fibrin deposition in various tissues by an antibody that specifically recognized the β-chain of fibrin, that becomes accessible after thrombin cleavage. In Sham mice treated with siAT low levels of fibrin deposition were present in the mammary fat pad (Fig. 3G, SFig. 2). However, a dramatic increase in fibrin deposition was found in tumors, 9-fold and 45-fold in MDA-231 + siNEG and + siAT treated mice respectively. Remarkably, fibrin deposition in the lungs was increased 15-fold in tumor bearing mice, either siNEG- or siAT-treated, when compared to Sham mice (Fig. 3H, SFig. 2). As these mice had lung metastasis, this suggests fibrin formation is mediated by the tumor and not by antithrombin knockdown. Furthermore, as reported previously [11], high fibrin deposits were detected in the liver in Sham+siAT mice and this was reduced in the MDA-231 + siAT group (Fig. 3I). Together, these data suggest that the presence of a tumor in combination with antithrombin knockdown has synergistic effects on fibrin deposition in the mammary fat pad, with reduced clinical signs coinciding with venous thrombosis.

4. Discussion

Development of thrombosis in cancer patients correlates with poor survival. Unfortunately, the underlying mechanisms remain poorly understood. In this study, we investigated the effects of an aggressive breast tumor in an acute and non-invasive procoagulant mouse model for thrombus formation. This study reveals that, surprisingly, the presence of an aggressive breast cancer has a protective effect against hemostatic abnormalities in mice upon lowering antithrombin levels. siRNA treatment had no effect on tumor characteristics, like tumor growth or circulating tumor cells. However, metastatic spread was increased in mice with lowered antithrombin levels. In addition, murine TF and TFPI levels were increased in the tumor stroma. Furthermore, platelet counts were elevated in tumor bearing mice. Increased white blood cell counts, together with elevated inflammatory markers from the tumor suggested a pro-inflammatory status in mice with breast tumors that was further elevated after injections with siAT.

This *in vivo* model has previously been described as a spontaneous thrombosis model [11,16]. Based on the data presented, our model suggests a consumptive coagulopathy that might also reflect a state of disseminated intravascular coagulation (DIC). DIC is one of the most extreme forms of dysregulated hemostasis and is characterized by hemorrhages and/or thrombosis concomitant with decreased platelet count, low fibrinogen levels, prolonged prothrombin time and increased fibrin deposition [22]. This extreme form of hypercoagulation presents in 5 % of all breast cancer patients and especially adenocarcinomas of the breast are frequently associated with increased risk of DIC [23]. Although the mechanism behind cancer-associated DIC has remained elusive, it is believed that it may have the same triggers as cancer-associated thrombosis, such as elevated Tissue Factor either on primary tumor cells or extracellular vesicles, and a pro-inflammatory status in patients [24]. However, we did not observe altered TF expression in the tumors, suggesting that CAT in this current mouse model is not driven by TF.

In contrast to our hypothesis, the presence of a tumor appeared to protect from clinical features in the head coinciding with venous thrombosis, although not statistically significant due to the small group size. Whole blood analysis revealed high platelet counts upon establishment of a tumor before the induction of spontaneous VTE. The platelet counts were above 1000×10^9 counts/L, which would mimic thrombocytosis in a human setting. Interestingly, thrombocytosis is associated with inflammatory breast cancer [25] and metastasis [26], both being present in our mouse model. As platelets in our model are not completely consumed upon tumor growth, it is tempting to speculate that thrombocytosis produces an outcome that rescues mice from hemorrhagic bleedings in our preclinical model.

Besides elevated platelet counts, mice with MDA-231 tumors showed increased levels of plasma fibrinogen that remained unaltered after siRNA treatment. Increased fibrinogen levels are considered a marker of systemic inflammation [27]. This is in line with our results, as mice showed 10-fold higher white blood cell counts prior to siRNA treatment. These cell counts were further increased after siRNA injections. Additionally, the tumors display a pro-inflammatory status with elevated levels of interleukins and TNFα. This can be caused by both platelets and breast tumor cells. However, the primers used in this study are human specific, and the contribution of platelets to these enhanced cytokine levels are not taken into consideration. Among these pro-inflammatory cytokines, IL1β and IL6 can increase fibrinogen expression levels [28,29]. Although the levels of these interleukins are increased in MDA-231 mice with siAT, in comparison to siNEG, there was no further increase of fibrinogen levels in tumor-bearing mice treated with siAT. Although speculative, perhaps this could be an indication of saturated fibrinogen in the plasma. Furthermore, elevated fibrinogen levels can contribute to enhanced metastasis, as was shown by Palumbo and coworkers [30–32]. In line, several other studies have indicated an association of elevated plasma fibrinogen with higher tumor grade and poor

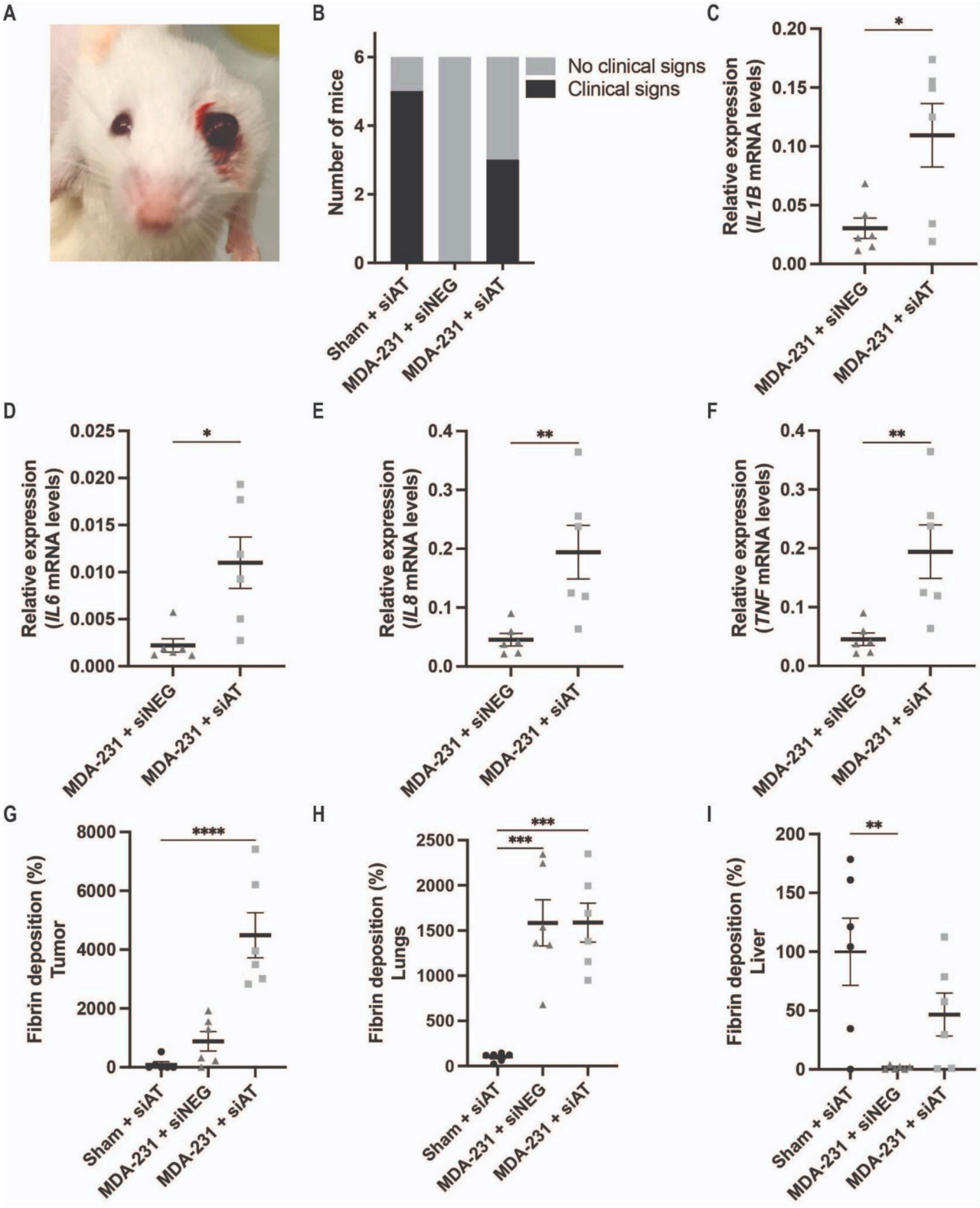

Fig. 3. The presence of an aggressive breast cancer tumor improves CAT score. (A) Clinical sign of bleeding in the left eye of a NOD-SCIDγ mouse 4 days post siAT injection. (B) Total number of mice that presented the clinical signs after 4 days of siRNA treatment ($n = 6$ per group). (C-F) mRNA expression levels of pro-inflammatory markers *IL1B* (E), *IL6* (G), *IL8* (H) and *TNF* (I) in tumors of mice injected with siNEG or siAT. (G-I) Fibrin deposition in the (G) tumor in tumor-bearing mice (n = 6) or mammary fat pad in the Sham group (n = 6), (H) lungs and (I) liver were analyzed western blot antigen levels using ImageJ. $^{*}P < 0.05$, $^{**}P < 0.01$, $^{***}P < 0.001$, $^{****}P < 0.0001$.

survival [33–36]. Previously, we established that near-complete (90 %) depletion of circulating neutrophils did not affect the onset or severity of thrombus formation in our siAT model [16]. Thus, according to our study, antithrombin knockdown results in increased fibrinogen and inflammatory cytokines in mice bearing breast tumors.

Previously, our group reported that fibrin deposition was increased upon siAT in non-tumor-bearing mice [11]. In the current study we have shown that fibrin deposition in the liver is also increased after siAT treatment in tumor-bearing mice. Interestingly, in the presence of a tumor less clinical signs and fibrin deposition products were detected in the liver after knockdown of antithrombin, although no significance could be reached. In contrast, a tumor and decreased plasma antithrombin synergistically increased fibrin levels in the mammary glands of mice when compared to Sham+siAT or MDA-231 + siNEG conditions. The reason for this drop in liver fibrin deposition and increase in tumor fibrin deposits remain unclear. Although speculative, this increased fibrin deposition may be formed by the tumor cells as these cells are known to activate platelets and thereby mediate fibrin formation. This latter may - on its turn - prevent attack by natural killer cells and promote survival of cancer cells in the blood circulation [32], although no effect on the number of circulating tumor cells was observed in the current study. Furthermore, fibrin deposits in the lungs were low in Sham mice, while the lungs of tumor-bearing mice displayed equal fibrin deposits, irrespective of siAT treatment. This might be explained by the selection of the breast cancer cell line for this study. To ensure an aggressive breast cancer condition in mice, MDA-MB-231-pcDNA-GFP-lung cells were selected. This cell line was originally derived from MDA-MB-231 cells that stably express GFP and was isolated from lung metastatic foci [21]. Therefore, it has a high preference of metastasis to the lungs, which may directly result in tumor-induced fibrin deposition in the lung. Our recent publication with longer siRNA treatment of fourteen days, albeit at a lower dose, showed no differences in tumor growth or metastasis [17]. In contrast, here, we show a 3–4-fold increase of lung micro-metastases in mice with lowered antithrombin levels, despite equal tumor volume and number of circulating tumor cells. Tumor analysis reveals increased mouse-specific TF and TFPI expression, indicating the role for the host microenvironment in the tumor to mediate micro-metastasis. This is in line with a study by Sierko et al., where TFPI expression was predominantly expressed at the interface between stroma and breast tumor cells [37]. In addition, TFPI in breast cancer was suggested to influence metastatic spread *via* the lymphatic system. This might explain differences in lung metastases of tumor-bearing mice treated with siAT, while the number of circulating tumor cells were similar to those in mice treated with siNEG. This suggests that antithrombin-triggered hypercoagulation may increase inflammation and TFPI expression in the tumor milieu and facilitate metastasis. However, further research is warranted to discriminate the role of coagulation factors in metastasis *via* blood- or lymphatic vessels.

Tumor expressed TF or TF^{+} extracellular vesicles are considered to be major players in cancer-associated thrombosis – including DIC. In our study we have used an aggressive breast cancer cell line that overexpresses TF. Based on literature, it was expected that plasma from mice with a tumor would be hypercoagulant, with increased FXa generation rate. Despite high TF content on our tumor cells, plasma analysis showed no differences in FXa generation (data not shown). In contrast with our findings, Hisada et al. reported increased FXa generation in mice bearing orthotopic pancreas tumors [38], although this is the only cancer type that is reported to show an association between TF^{+} extracellular vesicles and venous thromboembolism [39]. Therefore, it is unlikely that high amounts of circulating coagulant TF (extracellular vesicles) were present in this mouse model with an aggressive breast tumor.

According to Virchow's triad three components are of importance for the risk of VTE, *i.e.*: i) damaged or activated endothelium, ii) disrupted blood flow and iii) changes in blood composition [40]. In this acute and non-invasive hypercoagulant model all three components are affected. The presence of a tumor can compress vessels and thus change shear stress. Simultaneously, the tumor can activate endothelial cells and promote thrombosis and/or tumor progression (reviewed in Ünlü et al., 2024) [41]. Activated endothelial cells induce leaky vessels and promote secretion of various (pro-inflammatory) cytokines and chemokines, like IL1β and CCL1, to promote a systemic pro-inflammatory status [41,42]. Furthermore, both cancer and thrombosis are characterized by extensive inflammation, with activation of neutrophils, monocytes and macrophages, highlighting an important role for these immune cells in the crosstalk between cancer and VTE [43,44]. In line with this, increased white blood counts were observed in mice bearing a tumor, and after siRNA treatment. Since the hematology analyzer used in this study is unable to discriminate between various types of white blood cells, it would be of interest to determine the nature of the immune cells involved in future experiments, and elucidate their contribution to CAT in our model.

Although many experiments have been performed in animal models to mimic human disease, current mouse models for cancer and thrombosis do not accurately mimic human disease. The major caveat of mouse VTE models is that VTE in mice is induced through invasive surgical manipulations, for example by laser ablation of endothelial cells, complete vessel ligation [45], or creation of stenosis model through partial ligation of the vena cava. Our model consisted of immune-compromised Nod-SCIDγ mice, allowing to engraft a highly aggressive human breast cancer cell line to mimic tumor progression with elevated risk of CAT. Further directions to optimize murine models to study siRNA-induced CAT, would be to switch to syngeneic settings with murine breast cancer cells engrafted in immune-proficient mice. This will allow to study the role of natural killer, B- and T-cells in thrombi. Of note, elevated activity of effector T-cells have been suggested to increase the risk of VTE in cancer patients treated with immune checkpoint inhibitors [46]. With this setup, another (yet important) influencer can be added to the complex mechanism of CAT: crosstalk between cancer, coagulation and immune cells. Moreover, the presence of a tumor significantly increased platelet counts in this study, platelets have been suggested to mediate cancer-associated thrombosis and inflammation [47].

Despite the relatively low risk of VTE in breast cancer patients, the overall incidence of VTE in breast cancer patients is high (18 % of all CAT cases) [48]. As the risk of breast cancer-associated thrombosis increases with metastatic burden, cancer treatment and surgery significantly impact VTE risk. Here, the scope of the study was to investigate the role of an aggressive breast cancer model in a non-invasive hypercoagulant mouse model. Despite the limitations of our hypercoagulant mouse model, we believe it is a good and non-invasive model to mimic CAT. Furthermore, we believe this model can be adjusted to investigate the effects of cancer therapy- and/or surgery-induced thrombosis in breast cancer.

In our work we also show that the presence of an aggressive breast tumor protects hypercoagulant mice - after knockdown of antithrombin - from severe consumption of blood clotting factors. These mice might possibly be rescued by elevated platelet counts. Due to the highly consumptive coagulopathy, it can be argued that this model presented here is a model for disseminated intravascular coagulation. The tumor introduces systemic changes in the blood leading to thrombocytosis, increased fibrinogen levels and inflammation, which may all be factors contributing to reduced clinical bleedings. Unfortunately, the underlying mechanism behind cancer-associated thrombosis or DIC in aggressive breast cancer is still not unraveled. Therefore, we propose further experiments in order to investigate and unravel the pathophysiological mechanism of breast cancer on thrombosis and/or DIC.

Funding

This study did not receive any external funding.

CRediT authorship contribution statement

Betül Ünlü: Writing – review & editing, Writing – original draft, Methodology, Formal analysis, Data curation, Conceptualization. **Marco Heestermans:** Writing – review & editing, Formal analysis, Data curation. **El Houari Laghmani:** Writing – review & editing, Formal analysis, Data curation. **Jeroen T. Buijs:** Writing – review & editing, Formal analysis. **Rob F.P. van den Akker:** Writing – review & editing, Formal analysis, Data curation. **Bart J.M. van Vlijmen:** Writing – review & editing, Formal analysis. **Henri H. Versteeg:** Writing – review & editing, Writing – original draft, Supervision, Methodology, Conceptualization.

Declaration of competing interest

The authors declare that they have no known competing financial interests or personal relationships that could have appeared to influence the work reported in this paper.

Appendix A. Supplementary data

Supplementary data to this article can be found online at https://doi.org/10.1016/j.thromres.2024.109200.

References

[1] R.L. Siegel, A.N. Giaquinto, A. Jemal, Cancer statistics, 2024, CA Cancer J. Clin. 74 (1) (2024) 12–49.
[2] C.E. DeSantis, et al., Breast cancer statistics, 2017, racial disparity in mortality by state, CA Cancer J. Clin. 67 (6) (2017) 439–448.
[3] S. Paneesha, et al., Frequency, demographics and risk (according to tumour type or site) of cancer-associated thrombosis among patients seen at outpatient DVT clinics, Thromb. Haemost. 103 (2) (2010) 338–343.
[4] M.B. Streiff, Thrombosis in the setting of cancer, Hematology Am. Soc. Hematol. Educ. Program 2016 (1) (2016) 196–205.
[5] Walker, A.J., et al., When are breast cancer patients at highest risk of venous thromboembolism? A cohort study using English health care data. Blood, 2016. 127(7): p. 849–57; quiz 953.
[6] D.P. Cronin-Fenton, et al., Hospitalisation for venous thromboembolism in cancer patients and the general population: a population-based cohort study in Denmark, 1997-2006, Br. J. Cancer 103 (7) (2010) 947–953.
[7] J.F. Timp, et al., Epidemiology of cancer-associated venous thrombosis, Blood 122 (10) (2013) 1712–1723.
[8] D. Kashyap, et al., Global increase in breast cancer incidence: risk factors and preventive measures, Biomed. Res. Int. 2022 (2022) 9605439.
[9] J. Ferlay, et al., Cancer incidence and mortality worldwide: sources, methods and major patterns in GLOBOCAN 2012, Int. J. Cancer 136 (5) (2015) E359–E386.
[10] I. Tikhomirova, et al., Interrelation of blood coagulation and hemorheology in cancer, Clin. Hemorheol. Microcirc. 64 (4) (2016) 635–644.
[11] H. Safdar, et al., Acute and severe coagulopathy in adult mice following silencing of hepatic antithrombin and protein C production, Blood 121 (21) (2013) 4413–4416.
[12] Y.K. Jongejan, et al., Atherothrombosis model by silencing of protein C in APOE*3-Leiden.CETP transgenic mice, J. Thromb. Thrombolysis 52 (3) (2021) 715–719.
[13] J.A. Diaz, et al., Critical review of mouse models of venous thrombosis, Arterioscler. Thromb. Vasc. Biol. 32 (3) (2012) 556–562.
[14] Y. Hisada, N. Mackman, Mouse models of cancer-associated thrombosis, Thromb. Res. 164 Suppl 1 (Suppl. 1) (2018) S48–S53.
[15] A.L. Palacios-Acedo, et al., Cancer animal models in thrombosis research, Thromb. Res. 191 (Suppl. 1) (2020) S112–S116.
[16] M. Heestermans, et al., Mouse venous thrombosis upon silencing of anticoagulants depends on tissue factor and platelets, not FXII or neutrophils, Blood 133 (19) (2019) 2090–2099.
[17] J.T. Buijs, et al., Assessment of breast cancer progression and metastasis during a hypercoagulable state induced by silencing of antithrombin in a xenograft mouse model, Thromb. Res. 221 (2023) 51–57.
[18] B. Kocaturk, H.H. Versteeg, Orthotopic injection of breast cancer cells into the mammary fat pad of mice to study tumor growth, J. Vis. Exp. 96 (2015).
[19] H.H. Truong, et al., beta1 integrin inhibition elicits a prometastatic switch through the TGFbeta-miR-200-ZEB network in E-cadherin-positive triple-negative breast cancer, Sci. Signal. 7 (312) (2014) ra15.
[20] B. Ünlü, et al., Genes associated with venous thromboembolism in colorectal cancer patients, J. Thromb. Haemost. 16 (2) (2018) 293–302.
[21] J.T. Buijs, et al., The direct oral anticoagulants rivaroxaban and dabigatran do not inhibit orthotopic growth and metastasis of human breast cancer in mice, J. Thromb. Haemost. 17 (6) (2019) 951–963.
[22] M. Levi, et al., Disseminated intravascular coagulation, Thromb. Haemost. 82 (2) (1999) 695–705.
[23] S. Sallah, et al., Disseminated intravascular coagulation in solid tumors: clinical and pathologic study, Thromb. Haemost. 86 (3) (2001) 828–833.
[24] D.I. Feinstein, Disseminated intravascular coagulation in patients with solid tumors, Oncology (Williston Park) 29 (2) (2015) 96–102.
[25] K. Harano, et al., Thrombocytosis as a prognostic factor in inflammatory breast cancer, Breast Cancer Res. Treat. 166 (3) (2017) 819–832.
[26] J.L. Sylman, et al., Platelet count as a predictor of metastasis and venous thromboembolism in patients with cancer, Converg Sci Phys Oncol 3 (2) (2017).
[27] C. Perisanidis, et al., Prognostic role of pretreatment plasma fibrinogen in patients with solid tumors: a systematic review and meta-analysis, Cancer Treat. Rev. 41 (10) (2015) 960–970.
[28] G.A. Tennent, et al., Human plasma fibrinogen is synthesized in the liver, Blood 109 (5) (2007) 1971–1974.
[29] T. Yamaguchi, et al., Involvement of interleukin-6 in the elevation of plasma fibrinogen levels in lung cancer patients, Jpn. J. Clin. Oncol. 28 (12) (1998) 740–744.
[30] J.S. Palumbo, et al., Fibrinogen is an important determinant of the metastatic potential of circulating tumor cells, Blood 96 (10) (2000) 3302–3309.
[31] J.S. Palumbo, et al., Spontaneous hematogenous and lymphatic metastasis, but not primary tumor growth or angiogenesis, is diminished in fibrinogen-deficient mice, Cancer Res. 62 (23) (2002) 6966–6972.
[32] J.S. Palumbo, et al., Platelets and fibrin(ogen) increase metastatic potential by impeding natural killer cell-mediated elimination of tumor cells, Blood 105 (1) (2005) 178–185.
[33] Y. Luo, et al., Elevated plasma fibrinogen levels and prognosis of epithelial ovarian cancer: a cohort study and meta-analysis, J. Gynecol. Oncol. 28 (3) (2017) e36.
[34] X. Zhang, Q. Long, Elevated serum plasma fibrinogen is associated with advanced tumor stage and poor survival in hepatocellular carcinoma patients, Medicine (Baltimore) 96 (17) (2017) e6694.
[35] S. Fan, et al., Association between plasma fibrinogen and survival in patients with small-cell lung carcinoma, Thorac Cancer 9 (1) (2018) 146–151.
[36] K.T. Hwang, et al., Prognostic influence of preoperative fibrinogen to albumin ratio for breast cancer, J. Breast Cancer 20 (3) (2017) 254–263.
[37] E. Sierko, et al., Expression of tissue factor pathway inhibitor (TFPI) in human breast and colon cancer tissue, Thromb. Haemost. 103 (1) (2010) 198–204.
[38] Y. Hisada, et al., Human pancreatic tumors grown in mice release tissue factor-positive microvesicles that increase venous clot size, J. Thromb. Haemost. 15 (11) (2017) 2208–2217.
[39] A.A. Khorana, et al., Tissue factor expression, angiogenesis, and thrombosis in pancreatic cancer, Clin. Cancer Res. 13 (10) (2007) 2870–2875.
[40] H.H. Versteeg, et al., New fundamentals in hemostasis, Physiol. Rev. 93 (1) (2013) 327–358.
[41] B. Ünlü, N. Joshi, J.M. O'Sullivan, Endothelial cell dysfunction in cancer: a not-so-innocent bystander, in: Bleeding, Thrombosis and Vascular Biology, 2024, p. 3.
[42] A.D. Blann, Endothelial cell activation markers in cancer, Thromb. Res. 129 (Suppl. 1) (2012) S122–S126.
[43] A. Rosell, et al., Neutrophil extracellular traps and cancer-associated thrombosis, Thromb. Res. 213 (Suppl. 1) (2022) S35–S41.
[44] Y. Komohara, et al., Involvement of protumor macrophages in breast cancer progression and characterization of macrophage phenotypes, Cancer Sci. 114 (6) (2023) 2220–2229.
[45] J.A. Diaz, et al., Choosing a mouse model of venous thrombosis, Arterioscler. Thromb. Vasc. Biol. 39 (3) (2019) 311–318.
[46] P.A. Klavina, et al., Dysregulated haemostasis in thrombo-inflammatory disease, Clin. Sci. (Lond.) 136 (24) (2022) 1809–1829.
[47] A.L. Palacios-Acedo, et al., Platelets, thrombo-inflammation, and cancer: collaborating with the enemy, Front. Immunol. 10 (2019) 1805.
[48] C.C. Kirwan, E.L. Blower, Contemporary breast cancer treatment-associated thrombosis, Thromb. Res. 213 (Suppl. 1) (2022) S8–S15.